
Application of Combined Monte Carlo and Molecular Dynamics Method to Simulation of Dipalmitoyl Phosphatidylcholine Lipid Bilayer

S. W. CHIU,¹ M. M. CLARK,¹ ERIC JAKOBSSON,¹
SHANKAR SUBRAMANIAM,¹ H. LARRY SCOTT²

¹*Department of Molecular and Integrative Physiology, Department of Biochemistry, UIUC Programs in Biophysics, Neuroscience, and Bioengineering, and Beckman Institute, University of Illinois, Urbana, Illinois*

²*Department of Physics, Oklahoma State University, Stillwater, Oklahoma 74078*

Received 4 January 1999; accepted 29 March 1999

ABSTRACT: We describe a new equilibration procedure for the atomic level simulation of a hydrated lipid bilayer. The procedure consists of alternating molecular dynamics trajectory calculations in a constant surface tension and temperature ensemble with configurational bias Monte Carlo moves to different regions of the configuration space of the bilayer, in a constant volume and temperature ensemble. The procedure is described in detail and is applied to a bilayer of 100 molecules of dipalmitoyl phosphatidylcholine (DPPC) and 3205 water molecules. We find that the hybrid simulation procedure enhances the equilibration of the bilayer as measured by the convergence of the area per molecule and the segmental order parameters, as compared with a simulation using only molecular dynamics (MD). Progress toward equilibration is almost three times as fast in CPU time, compared with a purely MD simulation. Equilibration is complete, as judged by the lack of energy drift in three separate 200-ps runs of continuous MD started from different initial states. Results of the simulation are presented and compared with experimental data and with other

Correspondence to: H. L. Scott; e-mail: physhls@okstate.edu

Contract/grant sponsor: National Institutes of Health; contract/grant number: GM54651

Contract/grant sponsor: National Science Foundation; contract/grant number: 96-31050

Keywords: configurational bias Monte Carlo; molecular dynamics; atomic level simulation; model membrane

Introduction

Recent experimental studies of lipid bilayers^{1–4} have produced detailed pictures of the structure of fluid phase lipid bilayers, at the level of mean positions and conformations of constituent molecular groups. Currently, the only complementary theoretical approach with this level of detail is computer simulation. The motivation underlying simulations of lipid bilayers is that, by doing simulations that are consistent with available experimental data, we gain a viable atomic level structural and dynamical picture of the system. This amount of information greatly exceeds the information that may be obtained from the necessarily more coarse-grained experiments. The excess information then represents the prediction of the simulation, namely a trajectory or a set of atomic level system configurations consisting of atomic coordinates and velocities. The prediction is derived from interaction potentials and other constraints that constitute the *model* system under simulation. Predicted velocities and coordinates, averaged over many simulation steps, are used to calculate macroscopic properties of the model, which can be directly linked to the macroscopic behavior observed in experiments. This wealth of additional predictive information can be used to test hypotheses used by investigators in interpreting data and in the design of new experiments. It can also be used by theorists to formulate better coarse-grained statistical mechanical models for membrane behavior.

Atomic level simulations of lipid bilayers of dipalmitoyl phosphatidylcholine (DPPC) and other lipid bilayers have been carried out by several groups over the past several years.^{5–15} Several reviews of simulation methods and results have been published.^{16–19} With current computer technology it is possible to obtain trajectories of several nanoseconds on a system of the order of ~ 100 DPPC molecules in excess water.^{10–12,14} Although this represents remarkable progress, the size of the systems studied remains very small and the trajectories are so short that many important motions in

the system, such as large-scale lateral diffusion or membrane bending or torsional oscillations, are not observable.²⁰

A major problem in systems as complex as lipid bilayers is reaching equilibrium in finite computational time scales. In less heterogeneous systems, such as proteins, it is possible to begin from crystal structure configurations that are similar to configurations in the natural environment and rapidly evolve the system to equilibrium using molecular dynamics (MD) or Monte Carlo (MC) methods. In lipid membrane systems, crystal structures are highly ordered, and therefore are far from equilibrium relative to the fluid-like physiological state. One approach to the equilibration problem is to start the system from an array of randomly disordered configurations designed to be representative of a fluid-phase equilibrated state.⁵ Starting from randomized configurations, MD simulations are then used to drive the system to equilibrium. Two problems complicate this approach. The large number of degrees of freedom may preclude a rational choice of initial configurations that represent equilibrium states. And, second, MD trajectories sample a very small configurational space in sub-nanosecond time scales, and hence unless the initial random configurations are fortuitously near equilibrium, the system would not converge to equilibrium in a reasonable computational time. Conventional MC methods are also unable to accomplish equilibrium in a reasonable number of configurational searches.

An alternative method, employed by Chiu et al.,¹⁰ starts from the ordered crystal structure and uses high-temperature MD to achieve disordering of the system. This approach also suffers from the inability of MD to rapidly evolve the disorder toward an equilibrium configuration in finite computational timescales. The disordered state here also could be far from the equilibrium configuration.

Siepmann and Frenkel developed a method that holds high promise for the efficient sampling of flexible-chain torsion space.^{21,22} This approach, called configurational bias Monte Carlo (CBMC), attempts to use MC steps for entire chains or

molecules that have a higher likelihood of producing energetically favorable conformations by “re-growing” chains segment-by-segment. For each segment, multiple possible positions are sampled, and one is chosen based on Boltzmann weights. At the end of the growth, the entire new chain conformation is accepted or rejected based on a composite weight. The ability of this method to sample “allowed” configurational space rapidly suggests its use in conjunction with MD for rapid equilibration from ordered or random configurations.

In this article we describe the results of simulation of a DPPC bilayer in excess water in which alternating MD trajectory calculations with a set of CBMC are employed in order to accelerate the equilibration of the bilayer. This procedure exploits complementary features of MD and CBMC. CBMC moves across energy barriers more readily and efficiently than MD or conventional MC. Efficiency is achieved via reduced degrees of freedom, focusing on important transitions in configuration space. In this way, CBMC is able to explore large regions of configuration space in a coarse-grained

fashion, with convergence to a Boltzmann distribution. On the other hand, MD explores local regions of configuration space more thoroughly than CBMC because it replicates the continuous motions of the system. MD is guaranteed to ultimately converge to a Maxwell–Boltzmann distribution for all degrees of freedom if either: (1) the simulation is started near equilibration; or (2) the simulation is carried out for a very long time. When these procedures are alternated, the CBMC calculation permits the system to make substantial conformational changes provided those changes are energetically reasonable, whereas the subsequent MD calculation explores the region of conformational space near the region that CBMC has moved. In our simulations, this procedure is analogous to a series of quasistatic thermodynamic changes in the system from an initial highly ordered state to a final, disordered, fluid state. MD moves produce the changes and, after each small change, the system is driven back toward equilibrium by CBMC moves. A diagram of the overall simulation strategy is shown in Figure 1.

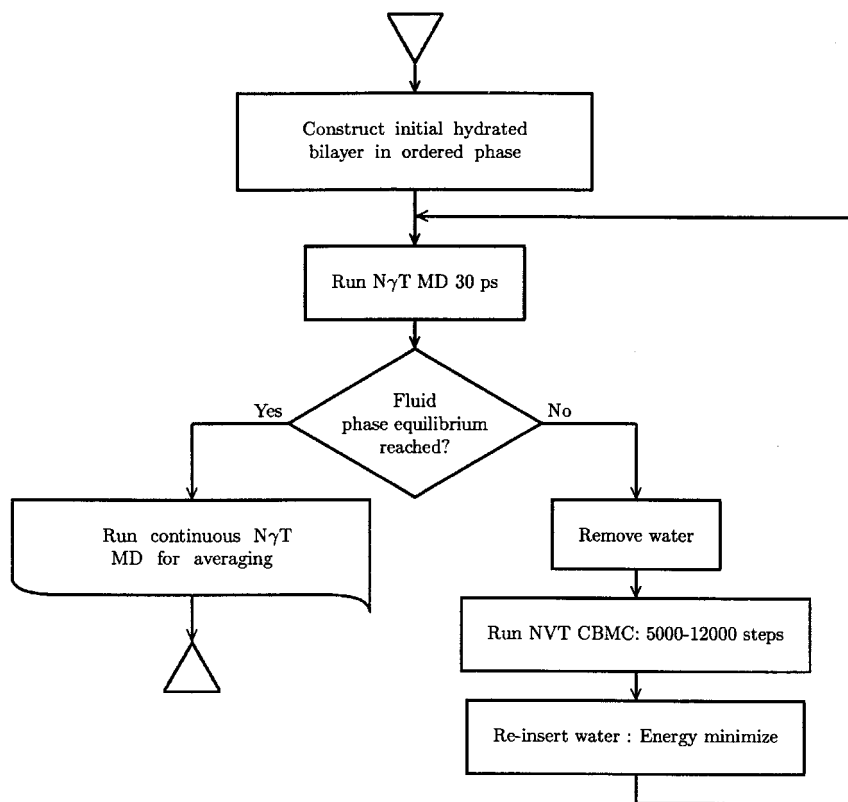


FIGURE 1. Flowchart of MD–CBMC procedure for generating an equilibrated fluid-phase bilayer from an ordered bilayer.

Simulation Strategy, Methods, and Procedures

We applied a combined MD–CBMC simulation procedure to a DPPC bilayer. The method utilizes MD in a constant surface tension and temperature ($N\gamma T$) ensemble,¹⁰ and CBMC in a constant volume and temperature (NVT) ensemble. Periodic boundary conditions are employed throughout. As a subject of many earlier simulations, DPPC is a good system on which to test our new procedure before moving to other applications. In our method, after a molecular dynamics simulation of 30 ps, run at constant temperature and constant surface tension, the system is subjected to a large number of CBMC moves at the same temperature and with the overall dimensions fixed at those corresponding to the time at which the molecular dynamics simulation was stopped. This approach allows the system to explore a local region of conformation space and to change its dimensions (if it is not equilibrated) during MD, and then to make significant conformational changes that are energetically reasonable during CBMC. When the final fluid-state equilibrium is reached, the area per molecule fluctuates about an average value during all subsequent MD runs. At this point, a continuous, uninterrupted MD run is used to calculate the average properties of the system.

The method is a variant of earlier hybrid simulation procedures used for lattice gauge theories and condensed matter systems.^{23,24} These methods utilize MC calculations as the basic simulation tool. The hybrid aspect is that each MC move is made using MD to evolve the entire system to a new state. The random nature of the move is due to random choices for initial velocities for each MD step (actually chosen from a Boltzmann velocity distribution). Although this is an appealing method it is not easily applicable to lipid bilayers. The short MD trajectory-based moves will not sample the wide range of lipid molecular configurations that are accessible to the system. Simulation of a system containing both lipids and water requires inclusion of fast-timescale motions such as water reorientations (MD) and slower configuration changes such as chain reorientations (CBMC).

We constructed a bilayer patch consisting of 100 DPPC molecules, 50 in each monolayer, and 3205 water molecules. The initial phase of the bilayer is the crystal structure, with coordinates of each lipid

TABLE I.
Summary of Continuous MD Runs.

Run	Starting Point	Duration	Temperature
Run I	605 ps	200 ps	325 K
Run II	715 ps	200 ps	325 K
Run III	925 ps	200 ps	325 K

generated from crystal-phase coordinates for DPPC.²⁵ Then, 30 ps of MD was run on this system using a temperature of 425 K. The MD was run using the $N\gamma T$ algorithm, which we employed in an earlier MD simulation of dimyristoyl phosphatidylcholine (DMPC) and DPPC.^{10,26} After the system reached an area per molecule that did not change systematically with time, the temperature was lowered to 325 K for further CBMC/MD cycles, until we judged the system had reached equilibrium. This occurred at a point when the total time for the MD runs was 925 ps. For the calculation of averages we then ran three separate continuous (uninterrupted by CBMC) MD trajectories of length 200 ps, starting from three different points in the completed equilibration run: the 605-ps point (run I); the 705-ps point (run II); and the 925-ps point (run III). Each trajectory was started after a CBMC run of 5000 steps and energy minimization. This procedure produced three separate, continuous $N\gamma T$ trajectories for averaging, and for testing the effects of the CBMC. Table I summarizes the three runs.

One change from the earlier simulation was the use of a longer cutoff for the van der Waals forces. Since our last published lipid simulations, we determined that the bilayer is not stable in a long simulation if the van der Waals cutoff is as small as 10 Å. We verified that liquid hexane is also not stable with such a short van der Waals cutoff. In this study a 20-Å cutoff is used for the van der Waals as well as the electrostatic interactions. Tu et al.¹¹ also recognized the significance of the long-range van der Waals cutoff for lipid simulations, in their case using a reaction-field correction for the long range van der Waals interactions. GROMOS²⁷ was used as the basic code package for the MD simulations, with our modifications for $N\gamma T$ constraints.^{10,26} We further experimented with different cutoffs for electrostatic interactions in the context of membrane simulations. The feature of the simulations we found to be most sensitive to the cutoff distance is the orientation of water molecules in the interfacial region, which

gives rise to the dipole potential. In earlier simulations of DMPC bilayers we found that the computed dipole potential was clearly incorrect when the cutoff for electrostatic interactions was 15 Å, but was reasonable when both 20- and 25-Å cutoffs were used. There was no significant difference in the results between simulations using 20-Å vs. 25-Å cutoffs for the electrostatics. We also experimented with Ewald sums in simulations of water, using both particle-mesh and more exact methods. In our experience, 20-Å cutoffs do not compromise the accuracy of the simulation, and are more efficient in regard to computational time.

After some initial experimentation with numbers of CBMC moves and lengths of intervening MD runs we settled on the following procedure. After each 30 ps of MD we ran 5000 CBMC steps. In the CBMC calculations, the water was not represented explicitly, and a dielectric constant of 80 was used for the electrostatic interactions between charged entities in the phospholipid molecules. The CBMC method has been described elsewhere.^{22,28,29} Each CBMC step in this simulation consists of the following procedure:

1. Cycle through the entire set of DPPC molecules. Do trial lateral translation and long-axis rotational moves for the entire molecule. Accept or reject by standard, Metropolis MC sampling procedures.
2. Pick a single DPPC at random, and pick one of the two chains, or the headgroup at random. Pick a bond on the chosen chain at random.
3. Generate 180 trial positions for the atom below the chosen bond (or above, in the case of headgroups). Calculate the configuration energy for each trial, and the weight, $w(n) = \sum_j \exp(-\beta E_j)$, where β is the inverse of Boltzmann's constant times the absolute temperature, and E_j is the energy of the atom at the j th trial position.
4. Pick one of the above trial positions with probability $\exp(-\beta E_j)/w(n)$.
5. Repeat the above process until the end of the chain is reached. Calculate the "Rosenbluth weight," $W(n) = \prod_{\text{atoms}} w(n)$.
6. Calculate the "old Rosenbluth weight," $W(o)$, of the initial configuration by repeating the above procedure with one of the trails being the original position of each atom.

7. Accept the new configuration of the chain with probability:

$$p = \min[W(n)/W(o), 1]$$

8. If configuration is rejected, reset coordinates of chosen chain or headgroup to original values.

Seipmann and Frenkel²¹ have shown that the above procedure is consistent with the requirements that configuration averages over states selected by the CBMC procedure are consistent with equilibrium thermodynamic averages. The CBMC procedure is carried out at the fixed box dimensions from the previous MD trajectory, and at the same temperature as the MD run. In the CBMC calculations, water molecules are represented by their dielectric constant, rather than explicitly, in order to save computer time. After each CBMC run, explicit water molecules are reinserted and the system is energy minimized before restarting the MD.

The entire combined equilibration process may be viewed as a series of "quasistatic" steps in the thermodynamic sense. As in a textbook expansion of a system, the process is carried out in a large number of slow, small, steps so that equilibrium is never disturbed from the beginning to the end of the expansion. In experiments, such as monolayer expansions, one ideally expands or compresses the system by moving the monolayer barrier by a small amount, and then stopping the barrier motion to let the system equilibrate (or, simply, move the barrier very slowly, which is a limiting case of the stop-start procedure). In our case, the system moves from its initial volume toward a final fluid-phase volume in a series of MD steps. On the other hand, the majority of torsion angle transitions, and hence the largest changes in the hydrocarbon chain order parameters, take place during the CBMC steps. In this procedure, as we have implemented it, the CBMC is run in an NVT ensemble using the fixed box size and temperature from the end of the previous MD step. Both the MD and the CBMC moves move the system reversibly through its phase space.

The one point in our procedure where reversibility is not maintained is the energy minimization (EM) step, which is needed because waters are not included in the CBMC moves. After a

CBMC run there are generally a few bad van der Waals contacts between headgroup atoms and water molecules. Whereas the EM step is not limited to water molecule readjustments, in practice only water molecules move appreciable distances. Usually, a local energy minimum is found in a few hundred EM steps. Although this procedure compromises the reversibility of the total procedure, it is only a small perturbation, because only a few waters are moved, and it can be argued that water molecules will, in general, reequilibrate on a faster timescale than lipid headgroups. Because the perturbed waters are few in number, and are in contact with the reservoir of bulk water, energetically significant local perturbations are quickly damped during the MD steps that follow CBMC and energy minimization (EM). Figure 2 is a plot of potential energy vs. time for runs I, II, and III. The changes in line style in Figure 2 indicate the beginning and endpoints of each run. Figure 2 shows that, after equilibration, the system stabilizes quickly after CBMC runs and remains very stable during three independent 200-ps intervals of continuous MD, for a total of 600 ps.

Interaction parameters used are the same as those used in our earlier DMPC MD simulation.^{10,26} In the CBMC runs, electrostatic interactions were

modulated by the continuum dielectric constant of water. In this simulation we used the same partial charges and van der Waals parameters as in our earlier DMPC simulations, but smaller charge groups. Figure 3 shows the charge groups used in this study. (The issue of force-field parameter choices is currently under further investigation by our group (see Discussion), but is not the focus of this study, which instead reports a new simulation method.)

Results

Figure 4 shows the fully expanded, hydrated, fluid-phase DPPC bilayer that our simulation produced. The total simulation consisted of 1.53 ns of MD and 150,000 CBMC steps (including whole-molecule moves for each lipid at each CBMC step, for a total of 10^5 Metropolis MC moves in addition to the 150,000 CBMC moves). About 5% of the CBMC moves generated conformations that were eventually accepted. Although this acceptance percentage seems low, it is about an order of magnitude better than the acceptance percentage for conformational changes that can be obtained by conventional MC procedures.³⁰ Figure 5 shows the

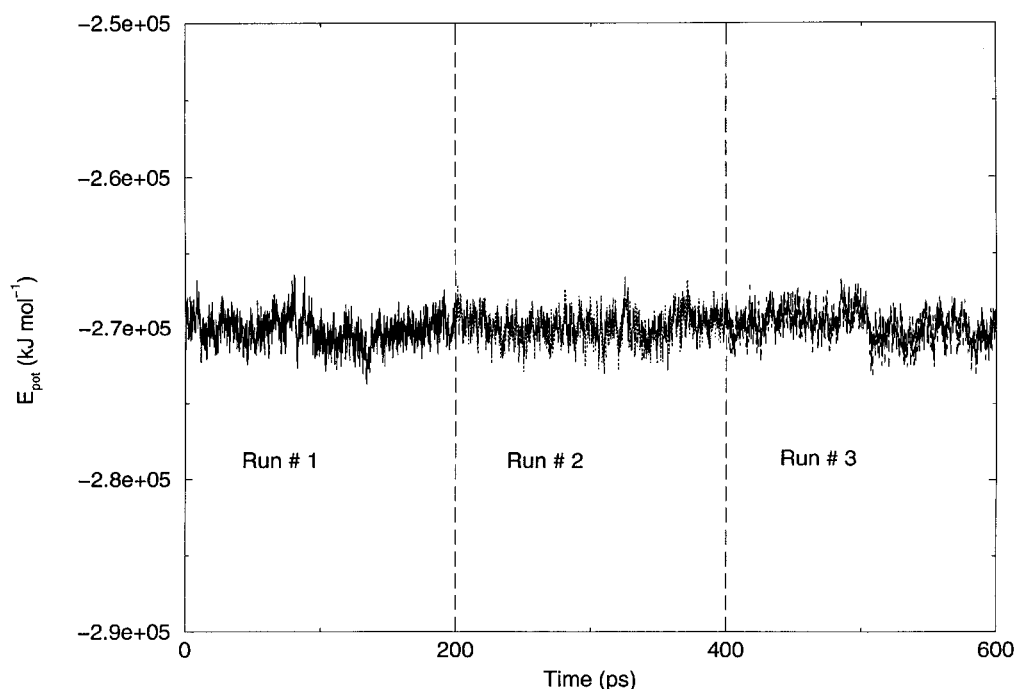


FIGURE 2. Plot of potential energy vs. time for MD runs started after CBMC and energy minimization (EM): 600-ps MD run with continuous segments of 200 ps interrupted by CBMC-EM. Line style changes denote points where CBMC-EM was run.

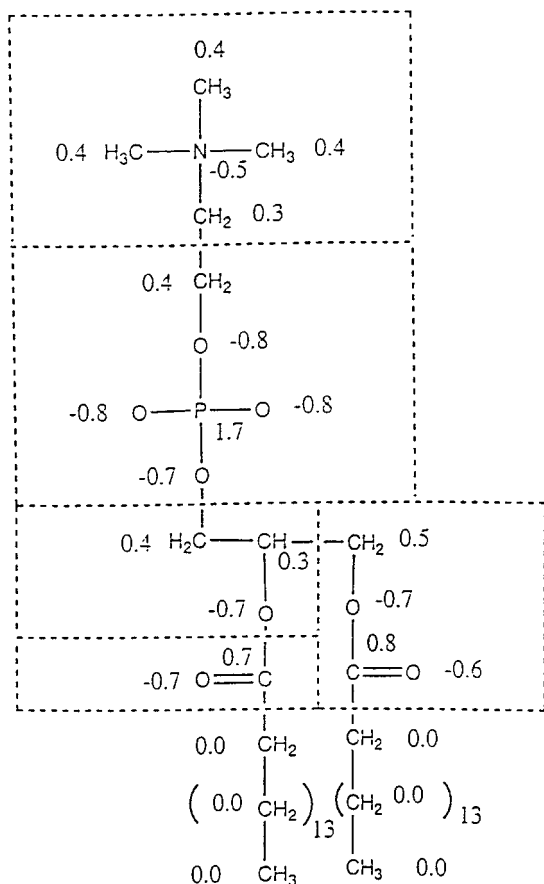


FIGURE 3. Charge distribution and charge groups used in the simulations. Numbers next to each atom represent partial charges in units of the electronic charge. Charge groups are outlined by dotted lines.

effect on equilibration of including CBMC moves by plotting the area per molecule vs. the MD simulation time for the MD-CBMC simulation and a simulation that used MD only, from the same initial state. The MD-CBMC simulation evolved much more quickly to the fluid phase. Each CBMC interval utilized about one third of the CPU time as the intervening MD runs. The slope of the dotted line in Figure 5a (representing MD/CBMC expansion) during expansion is about 3.5 times as great as the slope of the solid line (representing MD expansion) in Figure 5a. This gives a speed-up by a factor of about 2.6 in CPU time over MD for the expansion and equilibration of the fluid lipid bilayer.

Figure 6 shows the order parameter profile calculated from the 200-ps uninterrupted MD run at the end of the MD-CBMC expansion. The values for the order parameters near the chain tails ini-

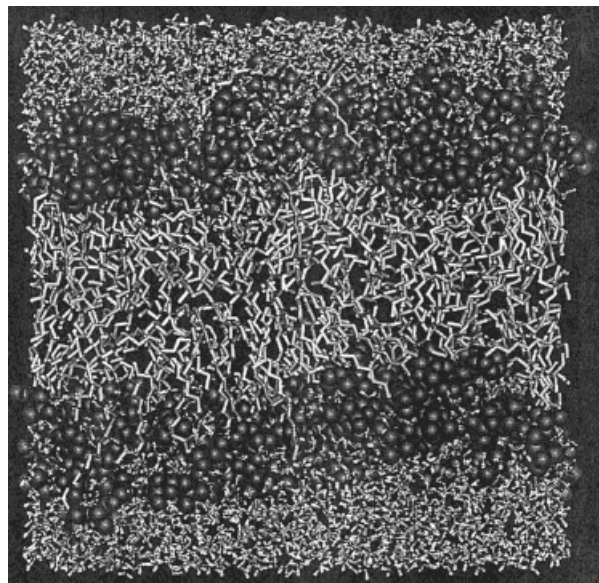


FIGURE 4. Snapshot of a fluid-phase DPPC bilayer after 1 ns of DPPC and 200,000 CBMC steps. Headgroup atoms are shown as balls, hydrocarbon chain bonds as thick sticks, and water molecules as thin sticks.

tially evolved to values about half of the experimental values, before converging to the data in the figure. This was due to our use of an elevated temperature during the equilibration phase of the simulation, and, also, to our use of reduced van der Waals repulsive parameters in the CBMC runs. The reduction in the van der Waals parameters was implemented to enhance disordering of the system, but we found, after about three iterations with this procedure, that slightly too much disorder was introduced in the chain tails. Because this change in parameter values disturbs the state of the system in a nonthermodynamic manner, it was subsequently abandoned, and, after about 600 ps, the parameters were reset to the correct values. Subsequently, the order parameters in the chain tails slowly increased in magnitude, approaching the experimental values from below. This "overshoot" illustrates the unanticipated efficiency of sampling the CBMC steps allowed in the hydrocarbon interior of the bilayer.

Figure 7 shows the effect of CBMC steps on different regions of the hydrocarbon chains. Figure 7a shows the evolution of $-S_{13}$, the order parameter at bond 13, for the Sn_1 chains. Each symbol on these figures represents the order parameter calculated from a single snapshot, either the final configuration of an MD run or the final configuration of a CBMC run. This adds "noise" to the data, but

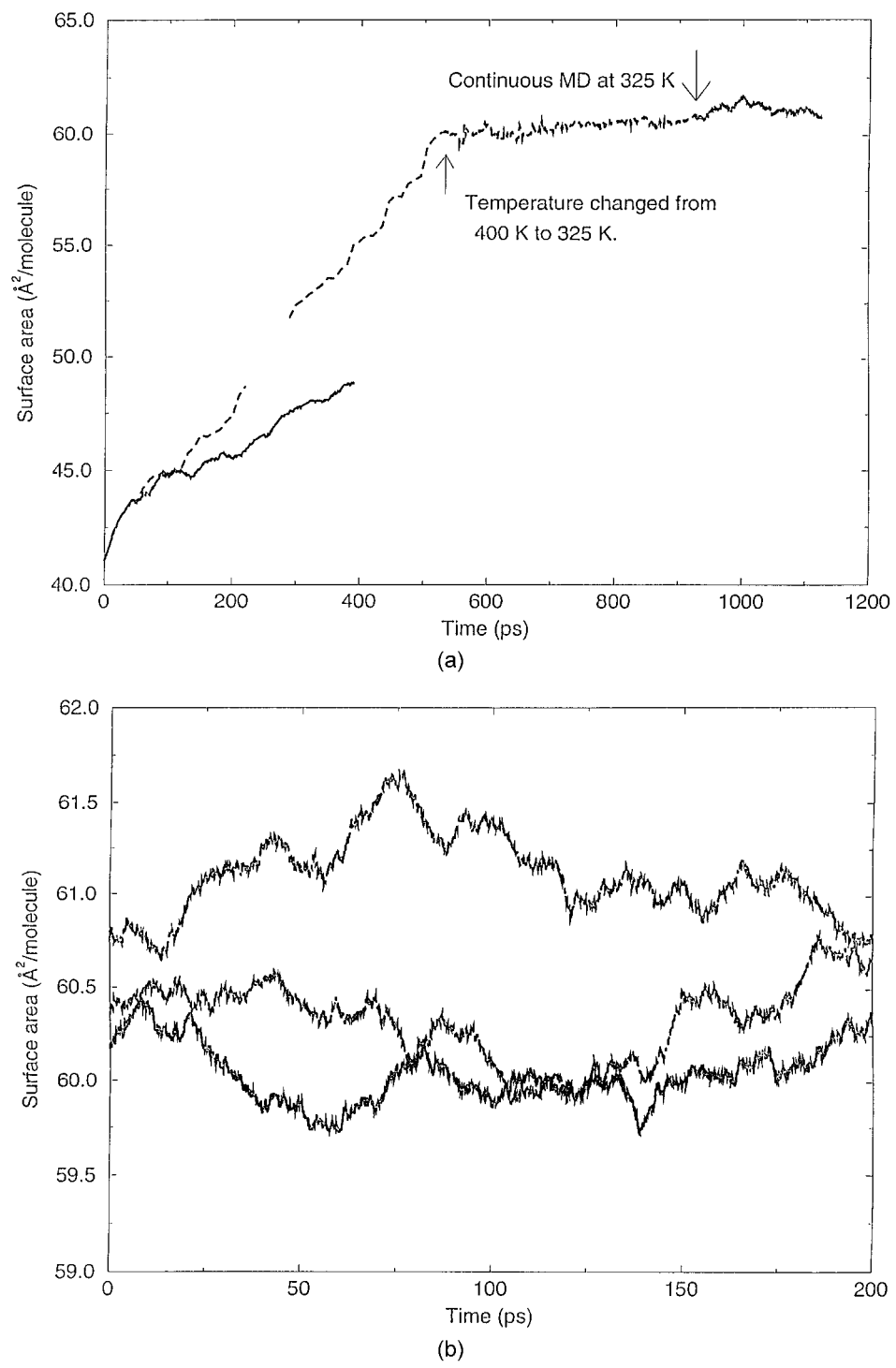


FIGURE 5. (a) Plot of the area per molecule vs. simulation time. Solid line: MD simulation (no CBMC steps). Dashed line: MD plus CBMC at elevated temperature (400 K); dot-dashed line: MD plus CBMC at 325 K (some data were lost from an early part of this run). These data include the expansion phase and the data from run I at the end. (b) Plot of area per molecule vs. time for runs I, II, and III. Top curve: run III; middle curve: run II; bottom curve: run I.

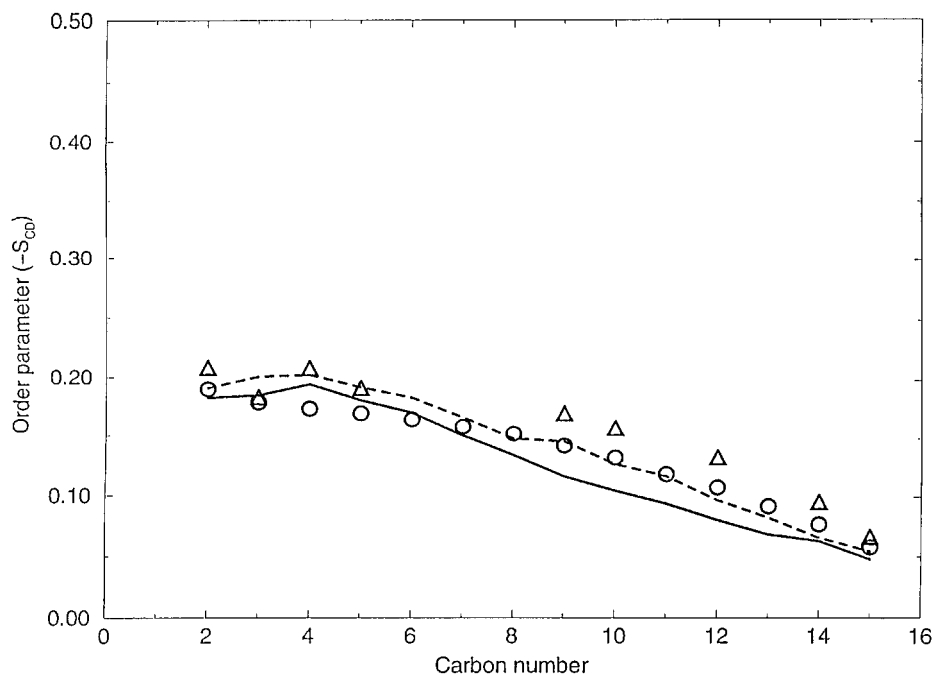


FIGURE 6. Plot of C—H order parameters vs. carbon number, averaged over the same data as Figure 2c. Solid line: S_{n1} chains; dashed line: S_{n2} chains. Triangles are data of Seelig and Seelig.³¹ Circles are data from McCabe et al.³²

more clearly illustrates the effect of combining CBMC and MD. The disordering effect of the CBMC steps is clear in Figure 7a. Figure 7b shows the evolution of $-S_3$, the order parameter at bond 3, for the S_{n1} chains. At the level of bond 3 the effect of the CBMC moves is less pronounced, but a disordering effect is still apparent. The behavior of the S_{n2} chains is very similar. The intermediate reduction of the van der Waals parameters does not appear to have affected the evolution of the chains at this level. In comparing the #3 carbon (Fig. 7a) with the #13 carbon (Fig. 7b), it is evident that the increased speed provided by CBMC in moving the system toward an equilibrated fluid phase manifests itself to a greater extent near the bilayer center; that is, near the methyl ends of the chains.

We have also calculated atom distributions for our DPPC bilayer. Figure 8 shows the atom distributions across the simulation cell. The natural symmetry of the distributions is indicative of the equilibration state of the lipids in the system. Figure 9 shows a plot of the average orientation of the P-N dipole vectors in the membrane plane vs. time for both the equilibrated fluid phase and the initial crystal state. The figure shows that, on average, P-N dipoles have not retained any of the order present in the initial, ordered lattice.

Discussion

The main conclusion to emerge from this simulation is that the combination of NVT molecular dynamics and configurational bias Monte Carlo is able to generate a fluid-phase lipid bilayer by guiding the system in a quasistatic equilibrium path through the configuration space. This path led to a more homogeneous and symmetrical bilayer than we have observed in the past using MD alone. Overall, about 5% of all CBMC are accepted, so that, in a CBMC run of 5000 steps, each lipid changes conformation of one of its chains or its headgroup two or three times. In addition, as described earlier, for each CBMC step, 100 whole-molecule MC moves consisting of translation or long axis rotation are attempted. The acceptance rate for these moves is also around 5%, leading to 250 accepted whole-molecule moves per lipid during a 5000-step CBMC run.

The effect of CBMC is primarily to alter configurations in the tail regions of the chains. Less frequently (about once per 500 CBMC steps), accepted new conformations may include changes in the upper regions of the chains or in the headgroups. Both the CBMC and the MD procedures

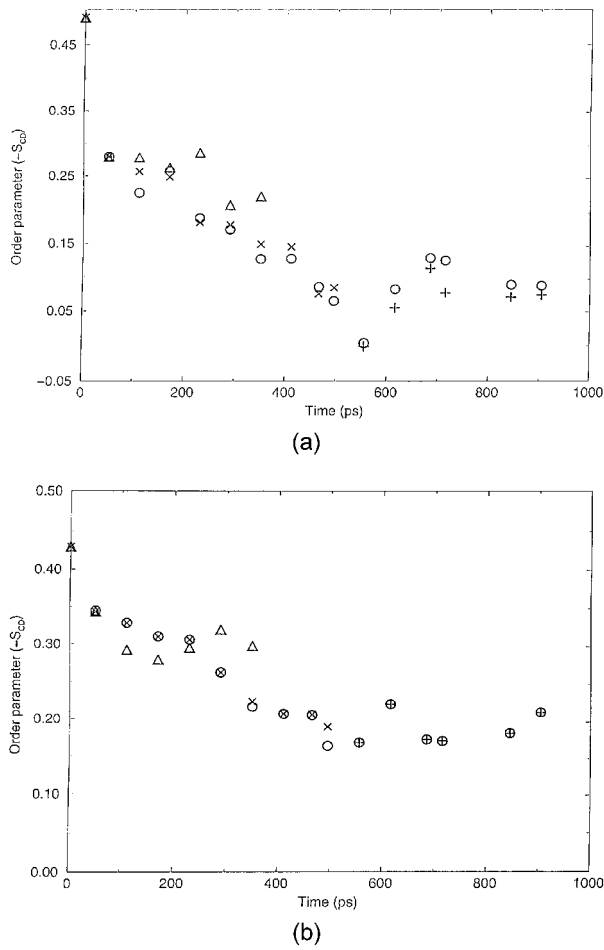


FIGURE 7. Evolution of order parameters for carbon 13 and carbon 3 vs. time. Triangles: MD simulation (no CBMC steps). (X) Order parameters at selected times immediately after 30 ps of MD at 400 K. (+) Order parameters at selected times immediately after 30 ps of MD at 325 K. Circles at same timepoints as X and +: order parameters after 10,000 CBMC steps from end of MD run. Where circles are not juxtaposed with X or +, CBMC has changed the order parameters from the values after the MD run. (a) Carbon 13: S_{n1} chains. (b) Carbon 3: S_{n1} chains.

tend to move the system toward a thermal equilibrium state. However, they do so on different scales of coarseness in conformational space, with the CBMC making coarse-grained moves and the MD more fine-grained moves. Our results suggest that the combined procedure is more efficient at ultimately finding an equilibrated state than either MD or CBMC alone, and give us confidence that the procedure may now be extended to more complex and more biologically relevant lipid bilayers. Although the major emphasis of this study is the successful application of the CBMC/MD pro-

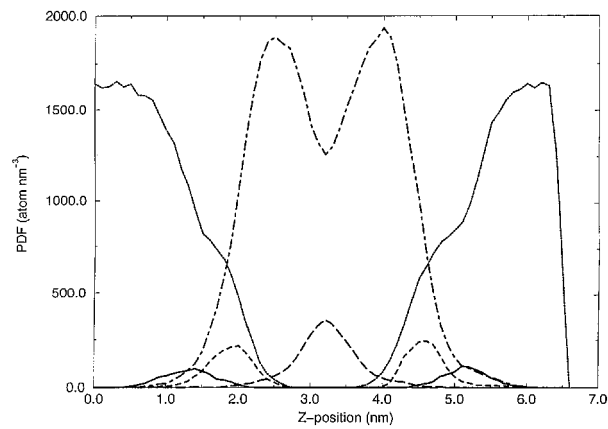


FIGURE 8. Atom distribution profiles across the bilayer, averaged over the combined data from runs I–III. Solid line: nitrogens; dashed line: carbonyl carbons; long dashed line: hydrocarbon chain terminal methyls; dotted line: water oxygens; dot-dashed line: hydrocarbon chain methylenes.

cedure to a DPPC bilayer, it is worth noting some issues related to the choices of parameters and boundary conditions for the simulations, and to make some comparisons with other relevant published simulations. With respect to the surface area per DPPC molecule, the result from this work is larger (61 Å² per molecule) than that for DMPC (58 Å²) in our previously published paper.¹⁰ This difference is partly due to the larger amount of water in the current simulation (32 waters per

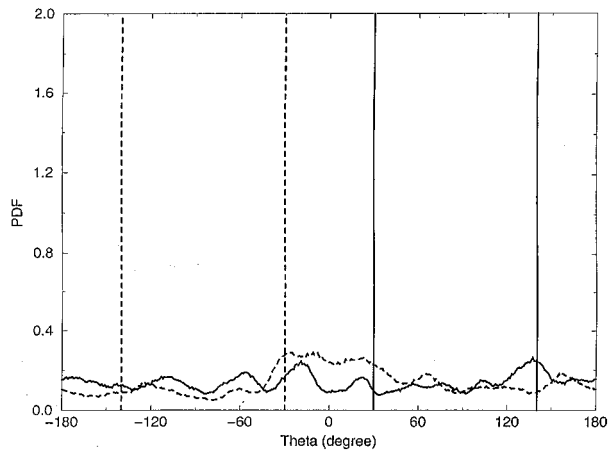


FIGURE 9. Plot of the probability density, binned in 1° intervals, of P–N dipole vector projection in the membrane plane as a function of time, averaged over the combined data from runs I–III. Sharp, δ -function-like peaks are orientations from both leaflets of the crystal structure used as the initial state for the simulation. Solid line: leaflet 1; dashed line: leaflet 2.

lipid, compared with 23 waters per lipid for the DMPC simulation). In a DMPC MD simulation subsequent to our published results, we found that increasing the hydration level from 23 to 32 waters/lipid increased the surface area/lipid by several square angstroms per molecule.²⁶ However, when we increased the van der Waals cutoff from 10 to 15 Å, we again obtained an area of less than 60 Å² per molecule in a pure MD calculation (unpublished results). We would now attribute this to our MD simulation not being able to achieve full equilibration in reasonable computation time, beginning in an ordered state.

In commenting on the effect of full hydration, we should point out a misconception that was inadvertently fostered in Figure 10 of our 1995 study.¹⁰ That figure suggests that water molecules at the surface of the membrane have approximately the same mobility as bulk water in a simulation with just 23 waters per lipid molecule. However, the comparison in that figure was made with water at 300 K, whereas the simulations were done at 325 K. So the correct inference from the simulations is that, with 23 waters per lipid, all of the water in the simulation is significantly less mobile than bulk water. With 32 waters per lipid the mobility of the water at the outer edge of the simulation cell is close to that of bulk water at 325 K.

The surface of the bilayer produced in our simulation is rougher than that reported by Berger et al.,¹³ as is apparent from comparison of snapshots from the two simulations (their Fig. 2 vs. Fig. 4). The difference in roughness also affects the width of the region from which water is excluded. This region is about 1.1 nm in width in Figure 8, compared with about 2 nm in the simulation of Berger et al.¹³ In general, the widths of distributions for all of the atoms in Figure 8 are greater than those shown in Figure 4 of Berger et al.¹³ Two possible reasons for these differences are the sizes of the two simulations, and degree of hydration. Berger et al. used a simulation cell with just 32 lipids per monolayer, whereas our simulation had 50. Berger et al. used just 23 waters per lipid, whereas we used 32. Both of these differences would tend to make the surface rougher and the spatial distributions of specific atoms wider in our simulations.

The simulations of Berger et al.¹³ utilized van der Waals parameters different from those used in this work. This affects the computed structure of the bilayer to some degree. Since the completion of the simulations described in this report we have begun a series of liquid alkane calculations with

the goal of optimizing the van der Waals parameters for lipid hydrocarbon methylene and methyl groups.³³ The simulations of Berger et al. were run with a cutoff of only 10 Å for the van der Waals interactions. In our ongoing simulations of liquid alkanes (unpublished) we established that a van der Waals cutoff of 10 Å is too short to maintain a liquid state of correct density in constant pressure simulations. A cutoff of 15 Å is sufficient to maintain this density, and a longer cutoff of 20 Å does not appreciably alter the results. Thus, the logical choice for the cutoff for van der Waals interactions for our N γ T simulations is 15 Å.

It should be noted that, because this is the first study that used the CBMC/MD combined method for equilibrating a biomolecular complex, some refinement of the method is to be expected in the future. The CBMC code is in an early stage of development, compared with the relatively mature MD code. For example, there is no inherent reason why the CBMC calculations could not be carried out in a constant pressure or surface tension ensemble, permitting the membrane area to change during the CBMC portion of the calculation as well as during the MD. Indeed, it might be advantageous to do so. However, because the capability to do this was already present in the MD code, for simplicity in the initial calculation we put the entire burden of adjusting the system dimensions on the MD section of the calculation. For membrane simulations, the CBMC algorithm appears to be highly parallelizable, which could make it possible to achieve extremely fast membrane equilibration on a massively parallel supercomputer. Even at the present stage of development of the CBMC code, the combined MD/CBMC moves toward equilibrium nearly three times as fast as pure MD, based on CPU time. It may also be that a more complete equilibration is achieved. Note in Figure 2 that there is no discernible drift in energy over 600 ps of MD simulation in the equilibrated system. In our previous simulations there were long, slow drifts in energy well into long MD simulations, which seemed to have been present in the simulations of lipid bilayers from other labs as well. If the code were made very parallel, it might be feasible to include explicit water molecules in the CBMC portion of the calculation if that were desired. However, the degrees of freedom associated with water molecules (molecular rotation, bond stretching, bond angle variation, and lateral translation) are more efficiently sampled by a separate MC or MD procedure. The CBMC method is designed specifically for determination of new

chain conformations; application to a small molecule, like water, is less efficient than using traditional Metropolis MC. In principle, it would be possible to design a totally MC simulation of a lipid bilayer using CBMC for the lipid conformations, and Metropolis MC for water and for lipid lateral translation and whole-molecule rotational moves.

Finally, we believe that a potentially important application of the MD/CBMC method is to the simulation of heterogeneous systems. In such systems, equilibration at interfaces can be problematic due to large barriers for the molecular motions which drive equilibration, for which CBMC may provide a means for hopping over or otherwise circumventing. For example, cholesterol poses significant steric barriers to the reorientation of neighboring lipid chains. We are currently using the MD/CBMC method to study lipid-cholesterol bilayers.

Acknowledgment

The authors thank V. Balaji for his contributions in optimizing the CBMC code.

References

1. Nagle, J. F.; Zhang, R.; Tristram-Nagle, S.; Sun, W.; Petrache, H.; Suter, R. M. *Biophys J* 1996, 70, 1419–1431.
2. Tristram-Nagle, S.; Petrache, H.; Nagle, J. F. *Biophys J* 1998, 75, 917–925.
3. Weiner, M. C.; White, S. H. *Biophys J* 1992, 61, 428–433.
4. Weiner, M. C.; White, S. H. *Biophys J* 1992, 61, 433–447.
5. Venable, R.; Zhang, B.; Hardy, B.; Pastor, R. *Science* 1993, 262, 223–226.
6. Stouch, T. *Mol Simul* 1993, 10, 335–362.
7. Egberts, E.; Marrink, S. J.; Berendsen, H. J. C. *Eur Biophys J* 1994, 222, 423–436.
8. Damodaran, K. V.; Merz, K. M. *Biophys J* 1994, 66, 1076–1087.
9. Feller, S. E.; Zhang, Y.; Pastor, R. W. *J Chem Phys* 1994, 103, 10267–10276.
10. Chiu, S.-W.; Clark, M.; Subramaniam, S.; Scott, H. L.; Jakobsson, E. *Biophys J* 1995, 69, 1230–1245.
11. Tu, K.; Tobias, D.; Klein, M. *Biophys J* 1995, 69, 2558–2562.
12. Teilman, D. P.; Berendsen, H. J. C. *J Chem Phys* 1996, 105, 4871–4880.
13. Berger, O.; Edholm, O.; Jahnig, F. *Biophys J* 1997, 72, 2002–2013.
14. Feller, S. E.; Yin, D.; Pastor, R. W.; MacKerrell, A. D., Jr. *Biophys J* 1997, 73, 2269–2279.
15. Husslein, T.; Newns, D. M.; Pattnaik, P. C.; Zhong, Q.; Moore, P. B.; Klein, M. *J Chem Phys* 1998, 109, 2826–2832.
16. Pastor, R. *Curr Opin Struct Biol* 1994, 4, 443–464.
17. Merz, K.; Roux, B., eds. *Biological Membranes: A Molecular Perspective from Computation and Experiment*; Birkhauser: Boston, 1996.
18. Teilman, D. P.; Marrink, S. J.; Berendsen, H. J. C. *Biochim Biophys Acta* 1997, 1331, 235–270.
19. Jakobsson, E. *Trends in Biochem Sci* 1997, 9, 339–354.
20. Pastor, R. W.; Feller, S. E. In: Merz, K. M.; Roux, B., eds. *Biological Membranes: A Molecular Perspective from Computation and Experiment*; Birkhauser: Boston, 1996.
21. Seipmann, I.; Frenkel, D. *Mol Phys* 1992, 75, 59–70.
22. Frenkel, D.; Smit, B. *Comput Phys* 1997, 11, 246–255.
23. Duane, S.; Kennedy, A. D.; Pendelton, B. J.; Roweth, D. *Phys Lett* 1987, 195, 216–222.
24. Mehlig, B.; Heerman, D. W.; Forrest, B. M. *Phys Rev* 1992, B45, 679–685.
25. Hauser, H.; Pascher, I.; Pearson, R. H.; Sundell, S. *Biochim Biophys Acta* 1981, 650, 21–51.
26. Chiu, S.-W.; Subramaniam, S.; Jakobsson, E. *Biophys J* 1996, 70, A94.
27. BIOMOS, Laboratory of Physical Chemistry, ETH Zentrum, Zurich, or see <http://igc.ethz.ch/gromos/>.
28. Scott, H. L. In: Merz, K. M.; Roux, B., eds. *Biological Membranes: A Molecular Perspective from Computation and Experiment*; Birkhauser: Boston, 1996.
29. Scott, H. L.; Jakobsson, E.; Subramaniam, S. *Comput Phys* 1998, 12, 328–334.
30. Scott, H. L. *Biophys J* 1991, 59, 445–455.
31. Seelig, J.; Seelig, A. *Q Rev Biophys* 1980, 13, 19–61.
32. McCabe, N. A.; Griffith, G. L.; Ehringer, W. D.; Stillwell, W.; Wassal, S. R. *Biochemistry* 1994, 33, 7203–7210.
33. Chiu, S.-W.; Clark, M.; Subramaniam, S.; Jakobsson, E.; Scott, H. L. Manuscript submitted.